

RESEARCH ARTICLE

Editorial Process: Submission:06/10/2024 Acceptance:10/21/2024

Competing Endogenous TMPO-AS1-let-7c-5p- LDHA RNA Network Predicts the Prognosis of Lung Adenocarcinoma Patients

Rajeev Nema¹, Prerna Vats¹, Jai Singh¹, Sandeep K Srivastava¹, Ashok Kumar^{2*}

Abstract

Objective: Lactate dehydrogenase is dysregulated in several cancer types. However, the mechanism of its dysregulation in lung cancer is not fully understood. We utilized web-based computational databases to conduct gene expression analysis on *LDHA*, identified its regulator, and explored their role in the prognosis of lung cancer. **Methods:** We used various web-based computational tools, including the UALCAN, TIMER2.0, ENCORI, TCGA Portal, OncoDB, and GEPIA2 datasets for lung cancer analysis in this study. We also performed survival, biological processes, and metastasis analysis using various computational tools. We also carried out co-expression functional enrichment analysis using the Enrichr and TIMER databases, multivariate analysis of survival and pathological stage, and transcriptional regulation analysis using the ENCORI and OncoDB datasets. Furthermore, LDHA inhibitor binding of withanolides was analyzed using Auto Dock Tools 1.5.6, LigPlot+, and Pymol. **Results:** The study found that the higher levels of *LDHA* gene expression were associated with poor prognosis and overall survival in lung cancer patients. We identified 11 key genes co-expressed with *LDHA*; out of them, two genes, MKI67 and PGK1, showed a strong positive correlation with *LDHA* and associated poor survival outcomes in LUAD patients. Furthermore, we also identified hsa-let-7c-5p and TMPO-AS1 as potential regulators of *LDHA* in LUAD. It might be possible that the TMPO-AS1- hsa-let-7c-5p-*LDHA* ceRNA network could serve as a potential regulator of aerobic glycolysis in LUAD and can serve as prognostic biomarkers. Further, Withanolides can inhibit the activity of LDHA and can be tested as an adjuvant treatment. **Conclusion:** We conclude that *LDHA* is overexpressed in LUAD, and the patients with high expression of *LDHA* exhibit poor prognosis. Further, the TMPO-AS1-hsa-let-7c-5p-*LDHA* ceRNA network can regulate aerobic glycolysis, thereby facilitating tumor growth in lung cancer.

Keywords: *LDHA*- TMPO-AS1- hsa-let-7c-5p- lung adenocarcinoma- E2F8- aerobic glycolysis- Withanolides

Asian Pac J Cancer Prev, 25 (10), 3673-3689

Introduction

Lung cancer is the most common cancer, with approximately 2.21 million confirmed cases and 1.8 million deaths recorded annually [1]. The main reason for the high mortality rate is that late diagnosis leads to poor outcomes. Histologically, lung cancer is divided into non-small cell lung cancer (NSCLC) and small cell lung cancer (SCLC); SCLC accounts for approximately 15% of all lung cancers [2]. NSCLC, which consists of 85% of all lung cancer, is further divided into lung adenocarcinoma (LUAD) and squamous cell carcinoma (LUSC) [3]. Smoking remains the most common risk factor for lung cancer [4, 5]. Conventional treatment modality is associated with increased resistance toward therapy and metastasis to distant organs.

Cancer cells demonstrate heightened aerobic glycolysis, also termed as 'Warburg effect'. Lactate dehydrogenase A (*LDHA*), which catalyzes the conversion of pyruvate to lactate, plays a crucial role in aerobic glycolysis and is recognized as a therapeutic anticancer target. *LDHA* catalyzes this process by converting pyruvate and NADH to lactate, which also contributes to epithelial-mesenchymal transition and metastasis [6]. *LDHA* plays a crucial role in cancer development and distribution, impacting the prognosis for cancer cells and the immune system. The role of *LDHA* in the prognosis of NSCLC has not been fully explored.

The tumor microenvironment is a complex ecosystem that includes many healthy or noncancerous cells, such as the immune system, signaling molecules, fibroblasts, and extracellular matrix [7, 8]. Hypoxia affects the

¹Department of Biosciences, Manipal University Jaipur, Dehmi Kalan, Jaipur-Ajmer Expressway, Jaipur, Rajasthan, 303007, India.
²Department of Biochemistry, All India Institute of Medical Sciences (AIIMS), Bhopal, Saket Nagar, Bhopal 462020, Madhya Pradesh, India. *For Correspondence: ashok.biochemistry@aiimsbhopal.edu.in. Rajeev Nema and Prerna Vats have equal contribution in this study.

oxygen supply from blood vessels, leading to the Warburg effect and excessive intracellular lactic acid production [9]. Excessive lactic acid production leads to protein denaturation and increased phospholipases, which damage cell walls and release lactic acid into the environment, thereby affecting neighboring cells [9-11].

Lung cancer is a heterogeneous disease, and the finding of new molecular prognostic markers is of utmost importance. Noncoding RNAs (ncRNAs), including long non-coding RNAs (lncRNAs), microRNA (miRNA), circular RNA (cirRNA), and piwi-RNA have been reported to regulate the tumorigenesis of numerous human cancers, including lung cancer. LncRNAs, when abnormally expressed, are linked to cancer development and influence gene expression, acting as microRNA sponges that affect cancer cell growth, proliferation, migration, and invasion. TMPO antisense RNA 1 (TMPO-AS1), a lncRNA, has been shown to promote the progression of NSCLC by regulating its natural antisense transcript TMPO [12, 13].

In this study, we investigated the role of *LDHA* and its ceRNA network as prognostic biomarkers. *LDHA* plays an important role in the growth and distribution of cancer and tumors that affect immunity. It inhibits glycolysis and reduces the oxygen demand of tumor cells, which is important in developing alternative cancer treatments [14]. The ceRNA network associated with *LDHA* controls the activity of genes involved in aerobic glycolysis, which leads to the Warburg effect in cancer cells [15]. This network includes various lncRNAs, miRNAs, and mRNAs that interact with *LDHA*, influencing its activity and expression levels to modulate the metabolic shift towards glycolysis. ceRNA interacts with *LDHA* to change its activity and expression levels, which in turn changes the metabolic shift toward glycolysis. Understanding the intricate interplay within this ceRNA network holds immense potential for identifying novel therapeutic targets and prognostic biomarkers in cancer patients. Naturally occurring C28 steroidal lactones with an ergostane-based skeleton have various biological activities, including antitumor activity [16]. The second objective of this study was to examine the inhibitory effect of withanolides on *LDHA*. This study aims to find a selective molecule, such as withanolide (withanolide D + NADH, withaferin A + NADH, withanolide O + NADH, withanolide E + NADH, withanolide G + NADH, and withasomnine + NADH), that targets LDH. We conclude that *LDHA* is overexpressed in LUAD and the patients with high expression of *LDHA* exhibit poor prognosis. Further, TMPO-AS1-hsa-let-7c-5p-*LDHA* ceRNA network can regulate aerobic glycolysis thereby tumor growth in lung cancer. Furthermore, we found that withaferin A and withanolide D bind to *LDHA* with a strength of -9.3 kcal/mol and -10 kcal/mol, respectively.

Materials and Methods

Expression analysis of *LDHA*

This study used publicly available databases to conduct gene expression analyses of lung cancer. Web-based computational tools, UALCAN (<https://ualcan.path.uab.edu>) [17], TIMER 2.0 (<http://timer.cistrome.org>) [18], and

Firehose Broad GDCA (<https://gdac.broadinstitute.org>) were used for pan-cancer analysis. Differential expression analysis of *LDHA* mRNA in lung cancer patients was determined using UALCAN, ENCORI (<https://rnasysu.com/encori/>) [19], TCGA Portal (<http://tumorsurvival.org/index.html>), OncoDB (<https://oncodb.org>) [20], and GEPIA2 (<http://gepia2.cancer-pku.cn/#index>) [21]. The relationship between *LDHA* expression and patient clinicopathological characteristics such as sub-type, lymph node status, smoking history, and methylation was analyzed using UALCAN.

Survival Analysis

We utilized the Kaplan-Meier Plotter (<https://kmplot.com/analysis/index.php?p=background>) [22] for survival analysis on lung cancer datasets by categorizing the patients with low expression and high expression data sets for target genes. The analysis included overall survival (OS), first progression (FP), and post-progression survival (PPS) using a Jetset probe. “Gene symbol, Affymetrix id: *LDHA*, 200650_s_at”; *MKI67*, 212023_s_at; *EIF2*, 201142_at; *ENO1L1*, 201231_s_at; *PGK1*, 227068_at; *PPIA*, 226336_at; *PSMD14*, 212296_at; *Gsp1*, 200749_at; *TPII*, 210050_at; *TUBA1C*, 209251_x_at; *VDAC1*, 212038_s_at; and *VDAC2*, 211662_s_at.

Functional Heterogeneity Analysis and Metastasis

CancerSEA (<http://biocc.hrbmu.edu.cn/CancerSEA/>) [23] was used to determine the correlation between *LDHA* gene expression and various biological processes. We used TNMplot (<https://tnmplot.com/analysis/>) [24] and ctcRbase (<http://www.origin-gene.cn/database/ctcRbase/index.html>) [25] datasets to analyze *LDHA*'s role in metastasis, and protein atlas (<https://www.proteinatlas.org>) [26] for protein expression analysis.

Co-expressed functional enrichment analysis

We identified *LDHA*-co-expressed genes using the Enrichr (<https://maayanlab.cloud/Enrichr/>) database [27] and investigated the relationship between *LDHA* and co-expressed genes in lung cancer using the TIMER (<https://cistrome.shinyapps.io/timer/>) database. We further validated the data using the TNMplot, GEPIA, and UALCAN databases.

Multivariate survival and pathological stages analysis

Using the KM plotter database, we conducted a mean gene expression multivariate survival analysis that included overall survival (OS), histology, smoking habit, and histology, along with smoking habit, using a Jetset probe. “Gene symbol, Affy id: *LDHA*, 200650_s_at”; *MKI67*, 212023_s_at; *PGK1*, 227068_at. We visualized the gene expression of the selected genes in different pathological stages using the GSCA (<https://guolab.wchscu.cn/GSCA/#/>) database [28].

Non-coding regulatory network analysis

We identified and validated miRNAs targeting the *LDHA* gene using the UALCAN database and ENCORI. We evaluated the prognostic significance of *LDHA*-associated miRNAs with pathological parameters

using CancerMIRNome and UALCAN. We utilized the atlas of non-coding RNAs in Cancer, LncTarD 2.0 (<https://lncatd.bio-database.com>) [29], ENCORI, and UALCAN for lncRNA analysis.

The transcriptional regulation analysis

We looked at the transcriptional factors that control the *LDHA* gene's function using the ENCORI and OncoDB datasets. We also looked at their prognostic value using the KM Plotter, looking at OS, histology, and histology with smoking history (Affy ID: 219990_at; E2F8). Using the UALCAN database, the expression of E2F8 in LUAD was examined based on different cancer stages, the patient's race, smoking habits, and node metastasis status.

Protein and ligand data acquisition and molecular docking

Human *LDHA* crystal structure with bound pyrazole derivative (PDB ID: 5W8L) was used for in silico docking calculations. Pymol [30] software was used to prepare the structure for molecular docking. Inhibitor binding pocket was analyzed by comparing different *LDHA*-inhibitor complexes available in literature (PDB IDs: 5W8H, 5W8I, 5W8J, 5W8K, 5W8L). The chemical structures of six ligands were obtained from the PubChem database [31]. Structure minimization was done using UCSF Chimera [32]. Auto Dock Tools 1.5.6 [33, 34] was used to analyze binding interactions with the *LDHA* protein. Gasteiger partial charges were assigned to ligand atoms, while Kollman charges were used for the protein. Ten docked conformations were generated for each ligand, and the top two hits with a docking score greater than the known inhibitors were selected for further validation. The protein-ligand complex was visualized using UCSF Chimera and LigPlot+ [35].

Statistical Analysis

We analyzed *LDHA* gene expression using t-tests and online database models to compare tumors and tissues. We examined the relationship between *LDHA* gene expression and prognosis. *LDHA* performance heterogeneity and gene enrichment A log-rank test was used to compare survival rates, and the significance level was $P < 0.05$.

Results

LDHA expression in lung cancer: A Pan-Cancer Approach

First of all, we compared the expression of *LDHA* in tumors and normal tissues from various cancer types. As shown in Figure 1A-C, the expression of *LDHA* was highly elevated in tumors from multiple cancer types, including LUAD and LUSC. We found that patients with LUSC and LUAD exhibited higher levels of *LDHA* gene expression, with a 9-fold increase in expression between normal and cancerous tissue, using the UALCAN database. As shown in Figure 2A-B (LUAD, $P = 1.6 \times 10^{-12}$ and LUSC, $P = < 1 \times 10^{-12}$), a consistent pattern of overexpression was observed in lung cancer patients using various databases, including ENCORI (LUAD, $P = 1.2 \times 10^{-37}$ and LUSC, $P = 2.9 \times 10^{-40}$), TCGA Portal (LUAD, $P = 4.2 \times 10^{-86}$ and LUSC, $P = 2.5 \times 10^{-82}$), OncoDB (LUAD, $P =$

4.2×10^{-86} and LUSC, $P = 2.5 \times 10^{-82}$) and Gepia 2 ($P < 0.05$), as shown in Figure 2C-I. Furthermore, the *LDHA* gene was hypomethylated ($P = 7.1 \times 10^{-12}$) in tumor tissues, compared to normal (Supplementary Table 1).

Survival analysis and correlation of LDHA with clinicopathological status

Then, to assess the prognostic role of *LDHA* in NSCLC, the Kaplan-Meier graphs were plotted using the KM Plotter database. As shown in Figure 2J and Table 1, results indicated that NSCLC patients with higher *LDHA* expression had a poor prognosis, with a significant association with OS (HR = 1.54, 95% CI: 1.37-1.74, $P = 1.2 \times 10^{-12}$). *LDHA* exhibited higher prognostic value for determining OS in LUAD (HR = 1.7, 95% CI: 1.42-2.02, $P = 2.5 \times 10^{-9}$) compared to LUSC (HR = 1.23, 95% CI: 1.01-1.49, $P = 0.036$) (Figure 2J-O and Supplementary Figure 1A-D). Thus, we focused our further study on LUAD. Then, we plotted OS KM plots for *LDHA* gene expression in LUAD patients with different clinicopathological conditions, including gender, age, and smoking status. *LDHA* showed an association with OS, both the males and females, and smokers and non-smokers (Figure 2J-O)

The role of LDHA in metastasis is enriched by functional heterogeneity analysis

Analysis using CancerSEA demonstrates a strong association between *LDHA* gene expression and several biological processes, such as invasion, DNA damage, cell cycle, metastasis, DNA repair, and EMT (Figure 3A-G). Cancer cells are primarily associated with invasion, DNA damage, metastasis, and EMT, making them resistant to therapy and difficult to treat. However, a negative association was found between *LDHA* gene expression and apoptosis (Figure 3H-I). An increased *LDHA* level in lung cancer cells aids in metastasis and the transition from epithelial to mesenchymal cells, thereby achieving resistance to available therapies. However, we found a negative association between *LDHA* gene expression and apoptosis (Figure 3H-I), confirming its role as an oncogene in lung cancer patients. Furthermore, the ctcRbase and TNMplot databases confirm that *LDHA* plays a crucial role in the progression of metastasis and the proliferation of circulating tumor cells (Figure 3 J-K). The expression of *LDHA* was much higher in lung metastatic tumors, compared to primary lung tumors (Figure 3K).

Then, using Enrichr, we identified co-expressed genes associated with the *LDHA* gene in LUAD and LUSC. The top 11 genes associated with *LDHA* expression in LUAD were as follows: *MKI67*, *EIF2S1*, *ENO1*, *VDAC1*, *VDAC2*, *PGK1*, *PPIA*, *PSMD14*, *RAN* (*Gsp1*), *TPII*, and *TUBA1C*. We further validated these genes using the TIMER database for both LUAD and LUSC. We found a strong positive correlation (correlation > 0.35) between each gene and *LDHA* in LUAD patients (Figure 4A-B), underscoring the significance of *LDHA* in LUAD. We also validated the co-expression of *LDHA* and its associated genes using TNMplot, GEPIA, and UALCAN databases, revealing similar results (Supplementary Figures 2A-J, Supplementary Figures 3A-V, Supplementary

Table 1. Survival Analysis of LDHA in Lung Cancer

S.NO	Index		Patient Number	Hazard Ratio	CI	Log (P)	Survival in months		
							Low Expression Cohort	High Expression Cohort	
NSCLC									
1	OS		2166	1.54	1.37-1.74	1.20E-12	90	51	
	FP		1252	1.54	1.3-1.82	5.90E-07	25.73	12	
	PPS		477	1.02	0.83-1.25	0.87	13.45	13	
LUAD									
2	Histology	OS	1161	1.7	1.42-2.02	2.50E-09	108.97	63	
		FP	906	1.82	1.49-2.23	4.00E-09	33.13	12	
	Gender	Male (OS)		566	1.71	1.35-2.17	8.40E-06	99	55
		Male (FP)		461	1.75	1.33-2.3	5.30E-05	27	10.43
		Female (OS)		537	1.63	1.24-2.16	0.00049	108.97	86
		Female (FP)		445	2	1.48-2.71	4.40E-06	45	14
	Smoking History	Smoker (OS)		546	1.84	1.41-2.41	5.40E-06	48	21
		Smoker (FP)		516	1.46	1.13-1.9	0.0042	102	48.73
		Non-Smoker (OS)		192	2.19	1.18-4.04	0.01	88.7	49.4
		Non-Smoker (FP)		189	2.29	1.37-3.81	0.0011	69	25
		LUSC							
3	Histology	OS	780	1.23	1.01-1.49	0.036	63.03	46	
		FP	220	0.93	0.62-1.4	0.74	11.83	13	
	Gender	Male (OS)		514	1.17	0.93-1.46	0.19	52	43.83
		Male (FP)		185	0.97	0.63-1.5	0.89	10	13
		Female (OS)		213	1.38	0.91-2.1	0.13	95.5	68.6
		Female (FP)		35	0.8	0.24-2.68	0.72	21.42	89.3
	Smoking History	Smoker (OS)		244	1.22	0.84-1.76	0.3	78.9	65.1
		Smoker (FP)		57	0.43	0.17-1.04	0.053	12.55	62
		Non-Smoker (OS)		9	Not detected			-	-
		Non-Smoker (FP)		1	Not detected			-	-

Figures 4A-K, and Supplementary Figures 5A-T). We further evaluated the prognostic role of the *LDHA* co-expressed 11 genes, and found that 8 (*MKI67*, *EIF2S1*, *ENO1*, *VDAC1*, *VDAC2*, *PGK1*, *TPII*, and *TUBA1C*) out of 11 genes, along with *MKI67*, were significantly associated with OS of NSCLC patients (Table 2 and Supplementary Figure 6A-K). Additionally, we analyzed these genes in relation to OS and LUAD, revealing that five co-expressed genes (*MKI67*, *ENO1*, *VDAC2*, *PGK1*,

and *TUBA1C*) significantly correlate with poor survival outcomes of LUAD patients (Supplementary Table 2 and Supplementary Figures 7A-P). To assess the effect of confounding factors, clinicopathological conditions such as history of smoking, histology, and cancer stages were selected for multivariate analysis. *PGK1* (HR = 1.73, 95% CI: 1.12-2.66, P = 0.012), *TPII* (HR = 1.64, 95% CI: 1.2-2.66, P = 0.012), *TUBA1C* (HR = 2.07, 95% CI: 1.49-2.88, P = 1.1e-05), *VDAC2* (HR = 1.81, 95% CI: 1.31-2.52, P

Table 2. Prognostic Role of LDHA co-expressed Genes in Lung Cancer

S.NO.	Gene	Index	Patient Number	Hazard Ratio	CI	Log(P)
1	<i>MKI67</i>	OS	2166	1.52	1.35-1.71	4.70E-12
2	<i>EIF2S1</i>	OS	2166	1.15	1.02-1.29	0.023
3	<i>ENO1</i>	OS	2166	1.35	1.19-1.52	9.70E-07
4	<i>PGK1</i>	OS	1411	1.42	1.22-1.64	3.80E-06
5	<i>PPIA</i>	OS	1411	0.74	0.63-0.85	4.50E-05
6	<i>PSMD14</i>	OS	2166	1.09	0.96-1.22	0.17
7	<i>RAN (Gsp1)</i>	OS	2166	0.98	0.87-1.11	0.79
8	<i>TPII</i>	OS	2166	1.17	1.04-1.32	0.008
9	<i>TUBA1C</i>	OS	2166	1.47	1.3-1.65	2.20E-10
10	<i>VDAC1</i>	OS	2166	1.2	1.06-1.35	0.0033
11	<i>VDAC2</i>	OS	2166	1.54	1.36-1.73	2.00E-12

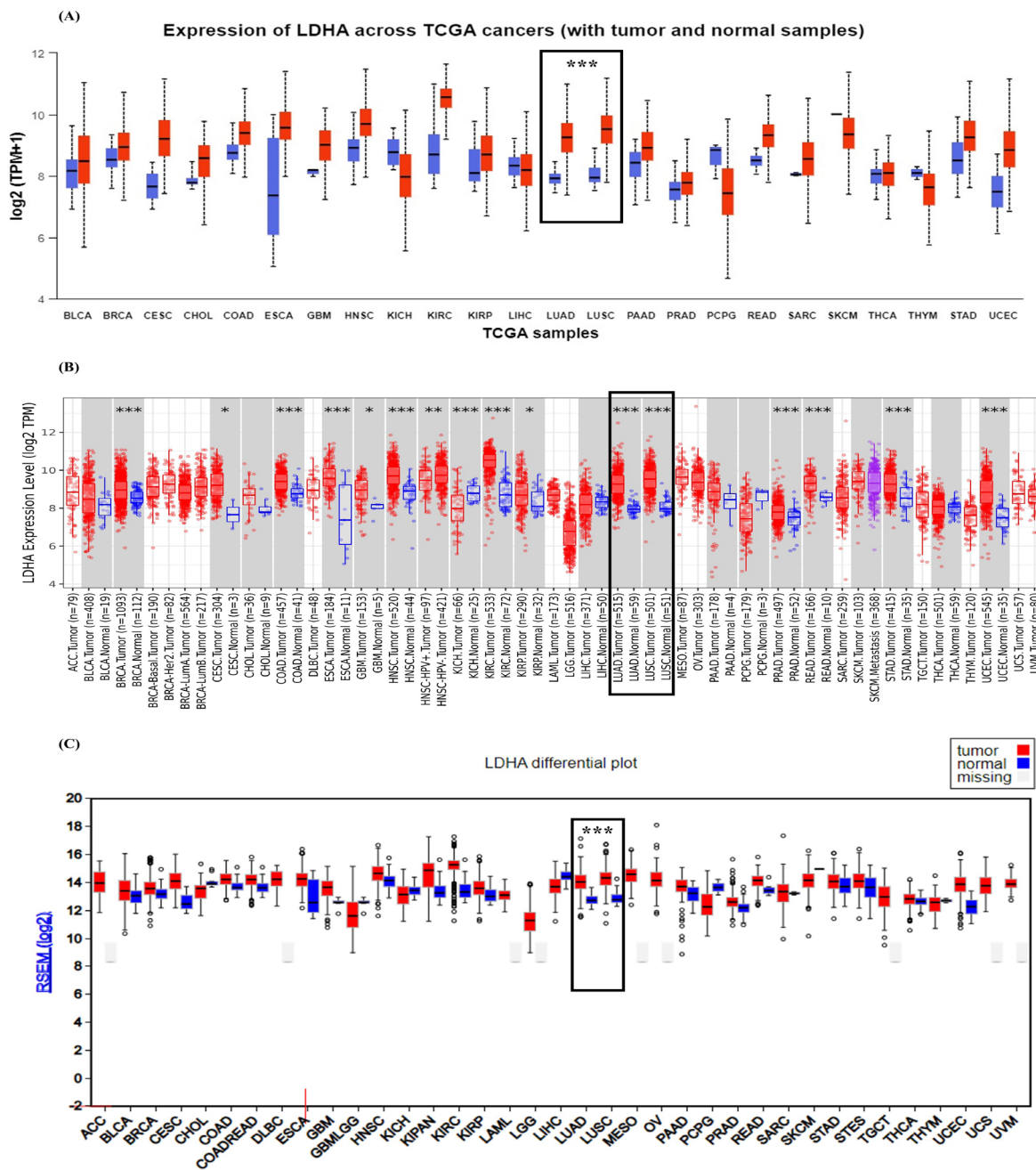


Figure 1. Expression Pattern of *LDHA* in Pan-Cancer (A) Expression profile of *LDHA* was determined by the UALCAN database for tumor versus normal samples; Red bars = Tumors, blue bars corresponding normal tissue. (B) expression of *LDHA* in pan-cancer by TIMER 2.0 meta-analysis; tumors compared with matched normal samples, red bar-dot plot = Tumors, blue bar-dot plot represents corresponding normal tissue. Error bars represent SD. ****p* < 0.001. (C) Pan-cancer analysis of *LDHA* expression using Firehose database, red bars indicates tumor and blue bars normal tissues.

Table 3. Expression Analysis of *LDHA* Co-Expressed Genes

S.NO.	Gene	Fold Change Tumor vs Normal
1	<i>LDHA</i>	1.6
2	<i>MKI67</i>	2.57
3	<i>PGK1</i>	1.55
4	<i>TUBA1C</i>	0.99
5	<i>TPH1</i>	0.97
6	<i>VDAC2</i>	1.09

= 0.00029), *MKI67* (HR = 1.87, 95% CI: 1.35-2.58, *P* = 0.00011), and *LDHA* (HR = 1.96, 95% CI: 1.43-2.71, *P* = 2.6e-05) showed high prognostic value in multivariate analysis (Supplementary Table 3 and Supplementary Figure 8 A–G). Importantly, LUAD patients with high protein levels of *LDHA* show poor survival outcomes compared to LUAD patients with low *LDHA* expression (Supplementary Figure 9A). Tumor tissues show high immunoreactivity for *LDHA* (Supplementary Figure 9B-C).

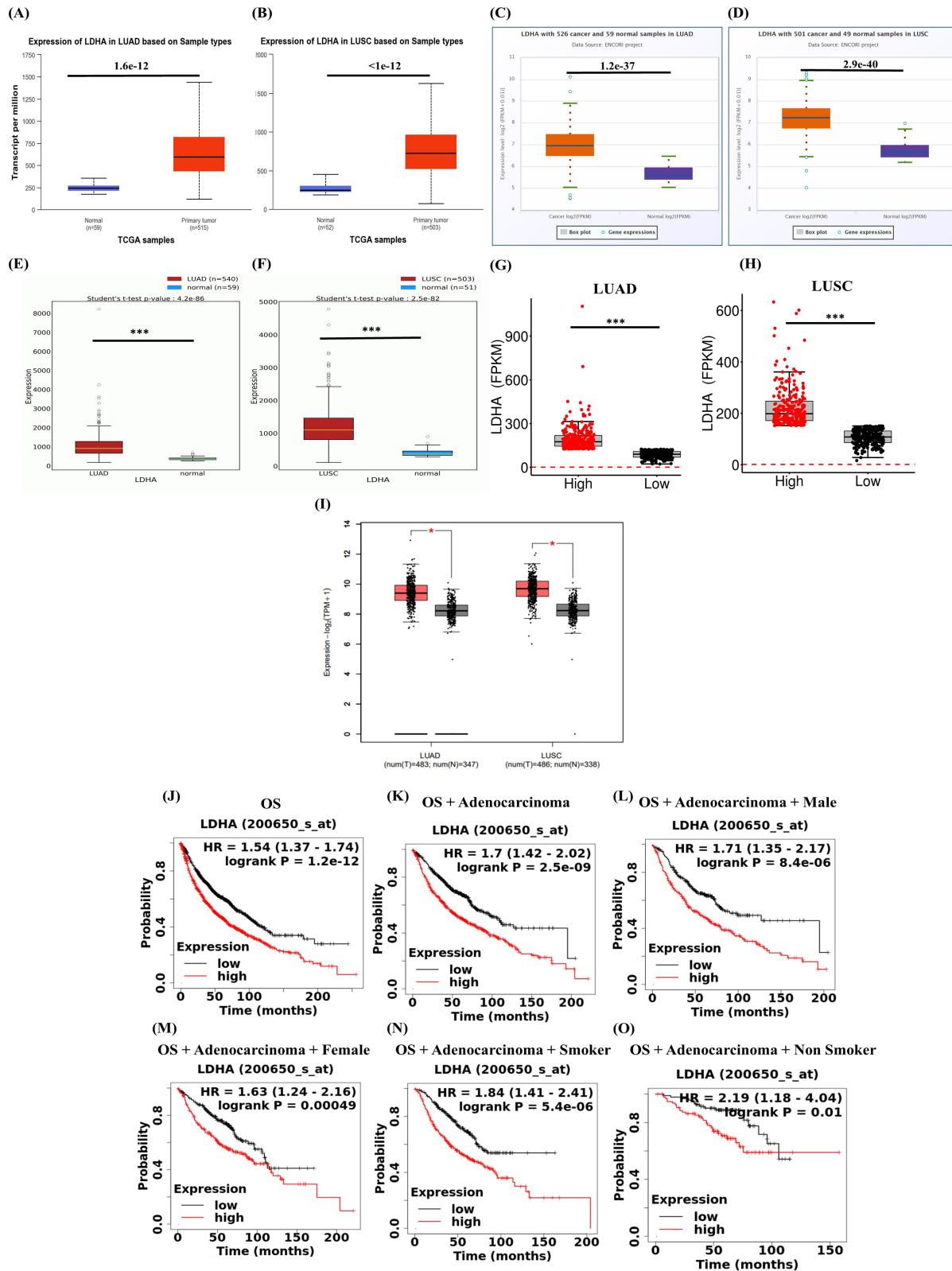


Figure 2. Expression of *LDHA* in Lung Adenocarcinoma (LUAD) and Lung Squamous Cell Carcinoma (LUSC) Patients. mRNA expression was analyzed in normal tissue and primary tumors from the publicly available databases using UALCAN (A) *LDHA* expression in LUAD (Normal n = 59, Tumor n = 515); (B) *LDHA* expression in LUSC (Normal n = 52, Tumor n = 503); ENCORI (C) *LDHA* expression in LUAD (Normal n = 59, Cancer n = 526); (D) *LDHA* expression in LUSC (Normal n = 49, Cancer n = 501); OncoDB (E) *LDHA* expression in LUAD (Normal n = 59, Tumor n = 540); (F) *LDHA* expression in LUSC (Normal n = 51, Tumor n = 503); TCGA portal (G) *LDHA* expression in LUAD; (H) *LDHA* expression in LUSC and GEPIA 2 (I) showing expression of *LDHA* in LUAD (Normal n = 347, Tumor n = 483) and expression of *LDHA* in LUSC (Normal n = 338, Tumor n = 486); (J-O) Prognostic role of mRNA expression of *LDHA* in lung cancer patients. Kaplan-Meier survival curves were plotted for overall survival (OS) in NSCLC patients (J) N=2166, lung adenocarcinoma patients (N=1161) (K), male lung adenocarcinoma patients (N=566) (L), female lung adenocarcinoma patients (N=537) (M), lung adenocarcinoma smoker patients (N=546) (N), and lung adenocarcinoma non-smoker patients (N=192) (O).

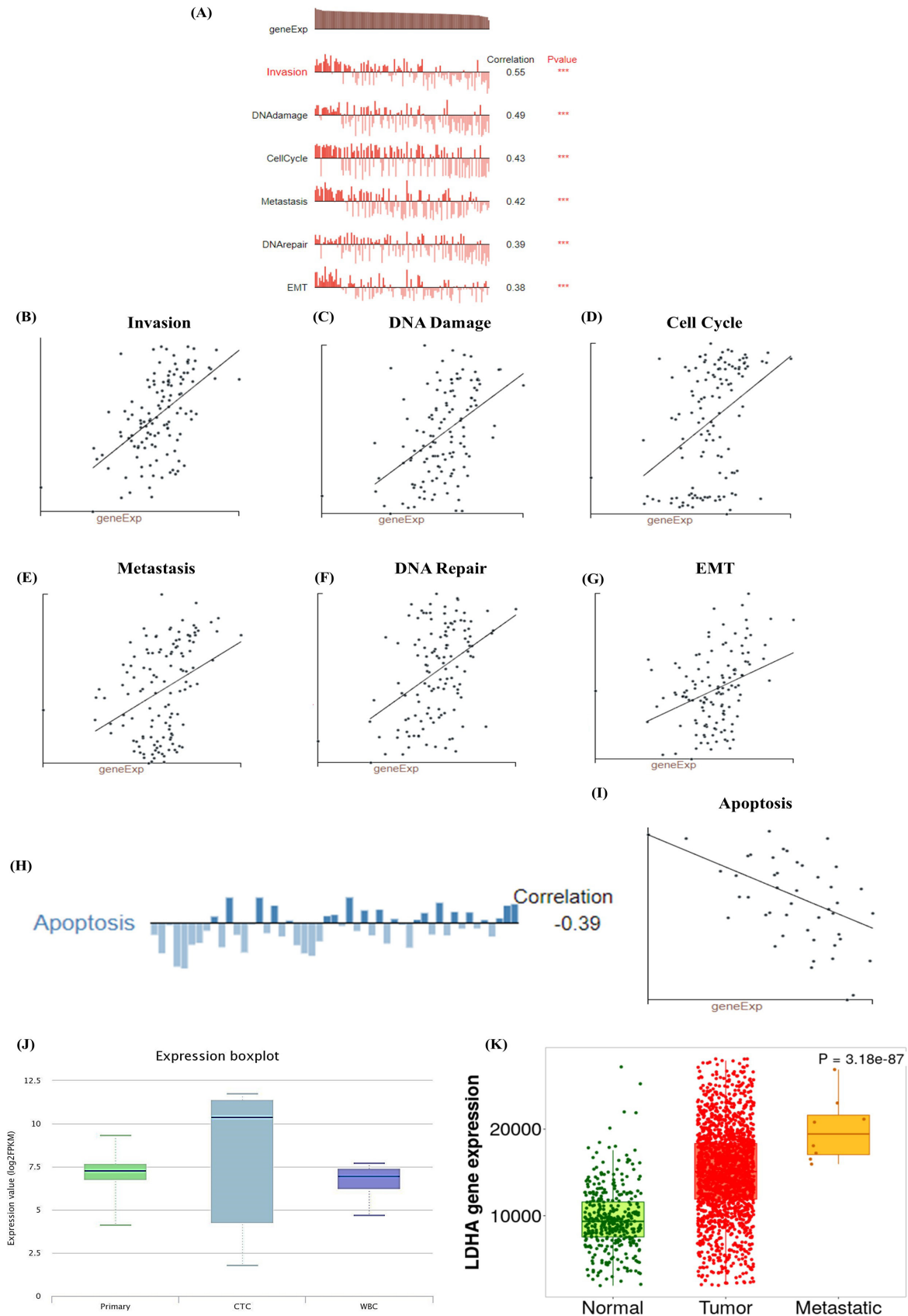


Figure 3. LDHA expression associate with (A) different biological processes and (B-G) showing a positive correlation with (B) Invasion, (C) DNA damage, (D) Cell cycle, (E) Metastasis, (F) DNA repair, (G) EMT and negative correlation with (H-I) apoptosis in lung cancer patients using the CancerSEA database; LDHA expression in tumors from lung cancer patients with metastasis. (J) Boxplot of LDHA expression in normal tissue, circulatory tumor cells (CTC), and WBC count from lung cancer patients using ctcRbase database. (K). Boxplot of LDHA expression between normal, primary lung tumor, and lung metastatic tissues using the Gene Chip- TNMplot database.

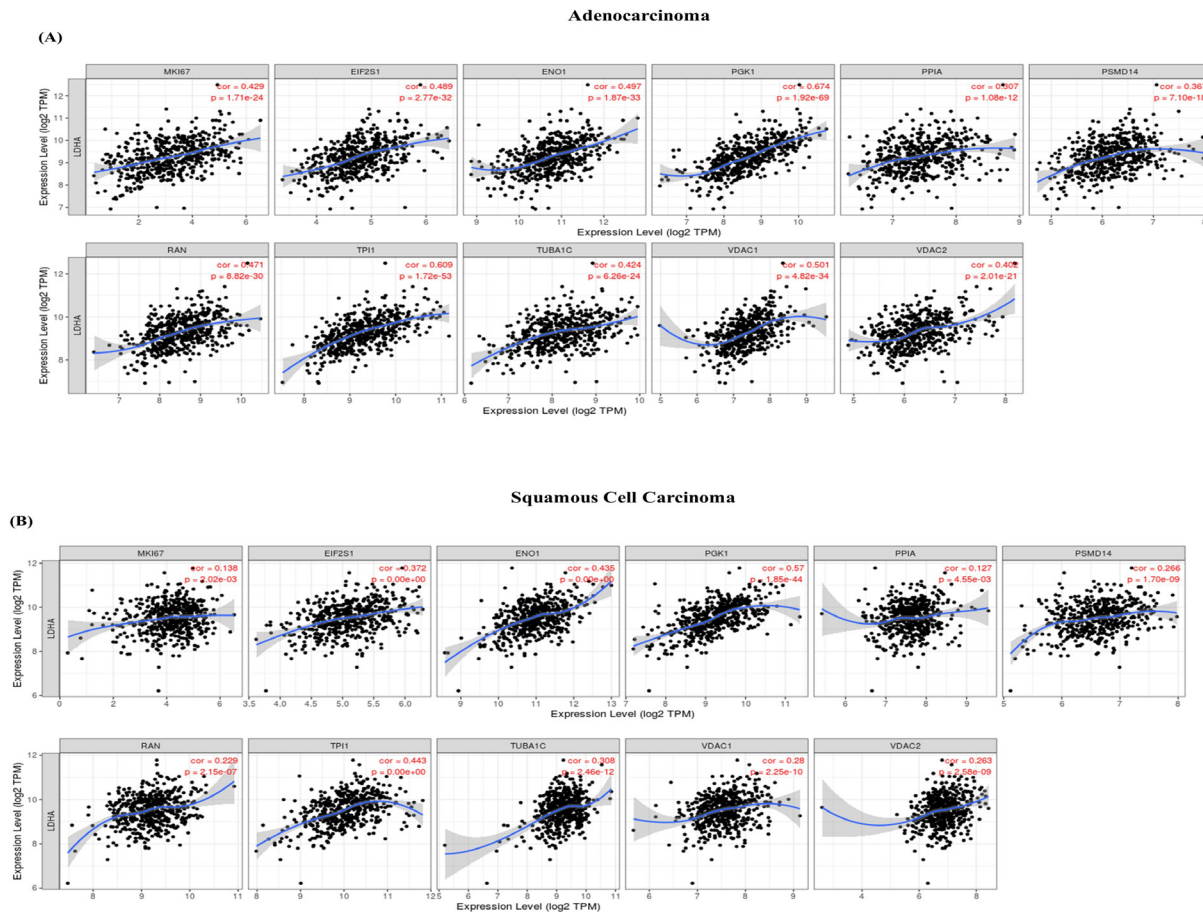


Figure 4. Expression Correlation between *LDHA* and Top 10 Co-Expressed Genes by Using TIMER 2.0. Expression Pattern of all co-expressed genes in (A) LUAD and (B) LUSC patients.

Furthermore, we compared the expression of co-expressed genes between tumor and normal tissue, and we found that *MKI67* ($F_c = 2.57$) and *PGK1* ($F_c = 1.55$), showed elevated expression in tumors from lung cancer patients (Table 3). Based on these results, we conclude that only *LDHA*, *MKI67*, and *PGK1* showed more than 1.5-fold consistent increased expression and were associated with the survival outcome of the LUAD patients, and thus, we chose these genes for further analysis. The study found a significant association for OS in NSCLC patients ($P < 0.05$) and a highly significant association with smoker LUAD patients (HR 3.14, $p = 1.3e-05$) (Table 4 and Figure 5A-D). Furthermore, we used the GSCA database to analyze the expression of the *LDHA*, *MKI67*, and *PGK1* genes in LUAD patients with different stages. Figure 5 E-G revealed a stronger association between the *LDHA* gene and stages with a false discovery rate (FDR) closer to 2.0, comparable

to *MKI67*, the gold standard biomarker for cancer cell proliferation. We observed a consistent expression pattern for *LDHA*, which increased with advancing stages, while the expression patterns of *PGK1* and *MKI67* were not consistent. The results suggest that *LDHA* can be a better progression biomarker for LUAD compared to *MKI67*.

Regulation of LDHA expression by microRNAs

LDHA dysregulation has been associated with a poor prognosis in several cancer types, but the mechanism of its dysregulation is unclear. miR-16-5p has been shown to regulate aerobic glycolysis by targeting *LDHA* [36]. Toward this, we analyzed the miRNAs that could target and regulate the expression of *LDHA*. Using the UALCAN database, we identified 16 downregulated miRNAs in tumors from lung cancer patients. These are hsa-mir-5588, hsa-mir-490, hsa-mir-1-2, hsa-mir-211, hsa-mir-99a, hsa-mir-29c, hsa-mir-548b, hsa-mir-4423, hsa-mir-101-1, hsa-

Table 4. Multivariate Overall Survival Analysis

S.NO.	Gene	Index	Patient Number	Hazard Ratio	CI	Log (P)
1	<i>LDHA + MKI67 + PGK1</i>	NSCLS patients	1,411	1.57	1.35-1.82	2.10E-09
		Adenocarcinoma	672	2.09	1.62-2.69	4.70E-09
		Smoker	330	1.95	1.32-2.87	0.00063
		Adenocarcinoma + Smoker	231	3.14	1.83-5.4	1.30E-05

LDHA + *MKI67* + *PGK1*

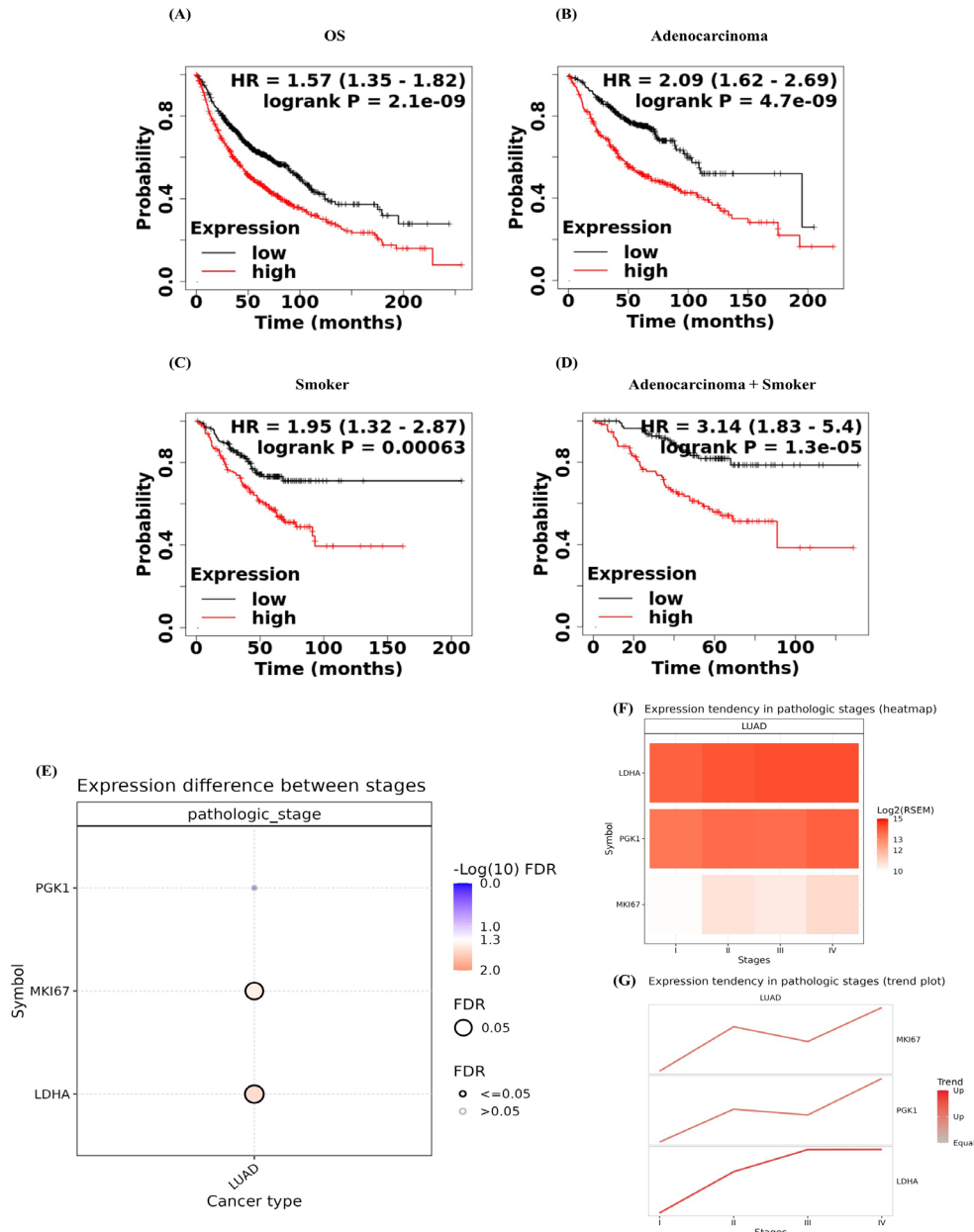


Figure 5. Prognostic Role of mRNA Expression of *LDHA*, *MKI67*, and *PGK1* in Lung Cancer Patients. Kaplan-Meier survival curves were plotted for (A) OS (n=1411), (B) Adenocarcinoma (n=672), (C) Smoker (n=330), (D) Smokers associated with adenocarcinoma (n=231); Expression pattern difference between stages using GSEA, (E) Difference in expression pattern of *LDHA*, *MKI67* and *PGK1* in lung cancer pathological stages, (F) heatmap showing expression tendency in pathological stages, (G) trend plot showing expression tendency in pathological stages.

Table 5. Association of *LDHA* with E2F Transcriptional Factors

S.NO.	E2F Transcription Factors	Coefficient R value	P value
1	<i>E2F1</i>	0.186	1.83E-05
	<i>E2F2</i>	0.207	1.60E-06
	<i>E2F3</i>	0.106	1.53E-02
	<i>E2F4</i>	0.115	8.13E-03
	<i>E2F5</i>	0.077	7.81E-02
	<i>E2F6</i>	0.074	8.91E-02
	<i>E2F7</i>	0.277	1.02E-10
	<i>E2F8</i>	0.328	1.29E-14

mir-584, hsa-mir-29a, hsa-mir-5680, hsa-mir-133a-1, hsa-let-30b, and hsa-let-7c. Using the ENCORI database, we analyzed the association of the above-mentioned miRNAs with *LDHA* and its co-expressed genes. Importantly, we found a significant negative relationship between hsa-let-7c-5p and the expression of *LDHA* ($r = -0.270$, $P = 5.22e-10$), *MKI67* (coefficient $R = -0.368$, $P = 6.82e-18$), and *PGK1* (coefficient $R = -0.226$, $P = 2.25e-07$) (Figure 6A-C). Furthermore, we found that hsa-let-7c-5p is significantly down-regulated in LUAD patients (Figure 6 D). Analysis with CancerMIRNome database showed a significant sensitivity and specificity for the decreased expression of hsa-let-7c-5p with an AUC value

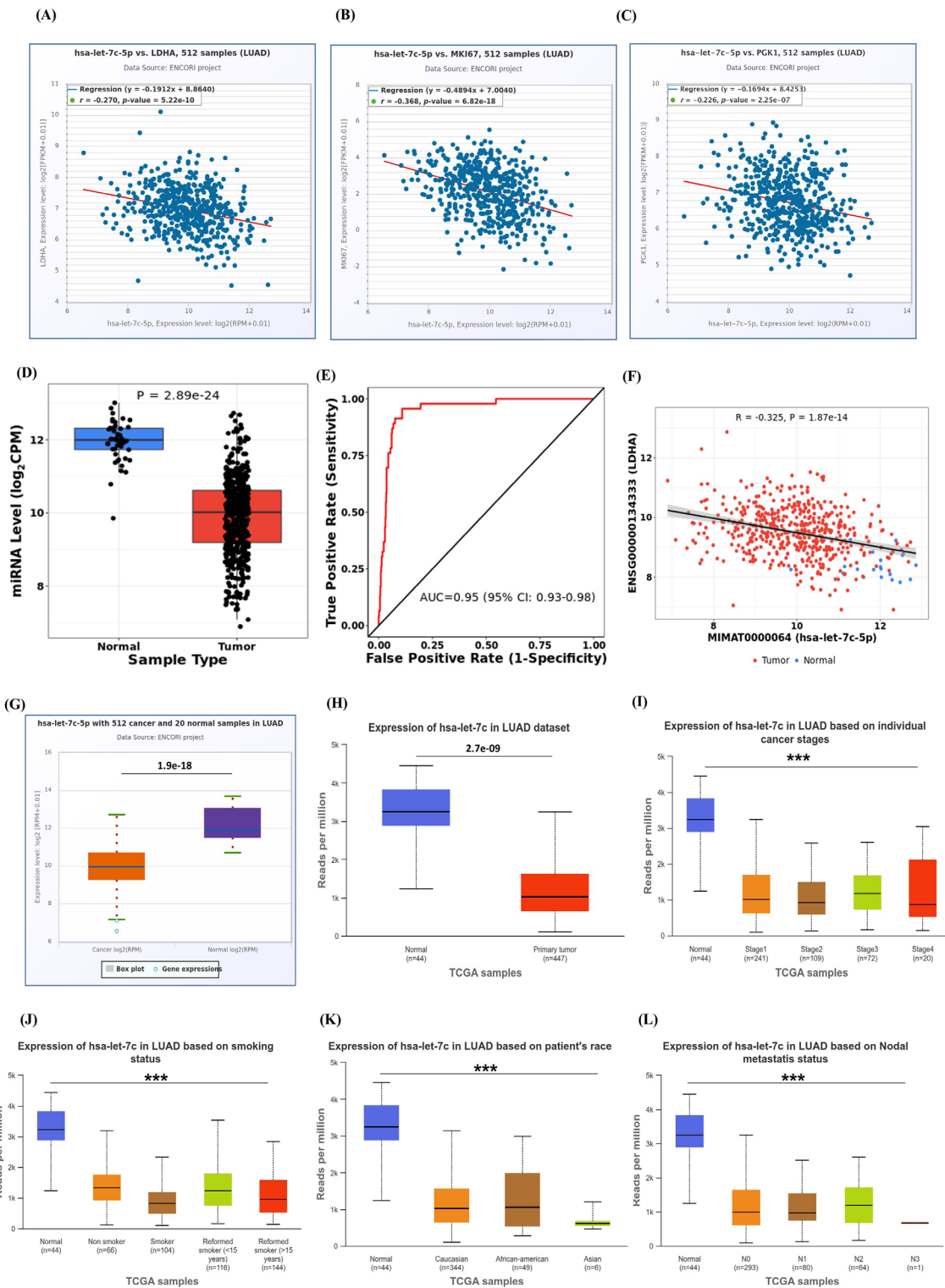


Figure 6. Co-Expression of miRNA and Gene in Lung Adenocarcinoma Samples, hsa-let-7c Showing Negative Correlation with (A) *LDHA*, (B) *MKI67*, (C) *PGK1* using ENCORI database; (D) Individual miRNA expression of hsa-let-7c in tumor tissues from lung cancer patients vs normal samples using CancerMIRNome, (E) ROC analysis curve showing specificity of hsa-let-7c in lung cancer patients (AUC=0.95) and (F) correlation between hsa-let-7c-5p and LDHA expression determined using CancerMIRNome. Validation of hsa-let-7c-5p downregulation in tumor samples as compared to normal by using (G) ENCORI and (H) UALCAN. Further, the UALCAN database to examine miRNA hsa-let-7c expression in LUAD based on (I) individual cancer stages, (J) smoking status, (K) patient's race, and (L) nodal metastasis status.

of 0.95 and a negative correlation with *LDHA* (Figure 6 E-F). Furthermore, the study validated the downregulation of hsa-let-7c-5p using the ENCORI and UALCAN

databases, revealing significant downregulation in LUAD patients, tumor cells, stages, nodes, races (Asian), and smokers (Figure 6G-L). The downregulation of hsa-

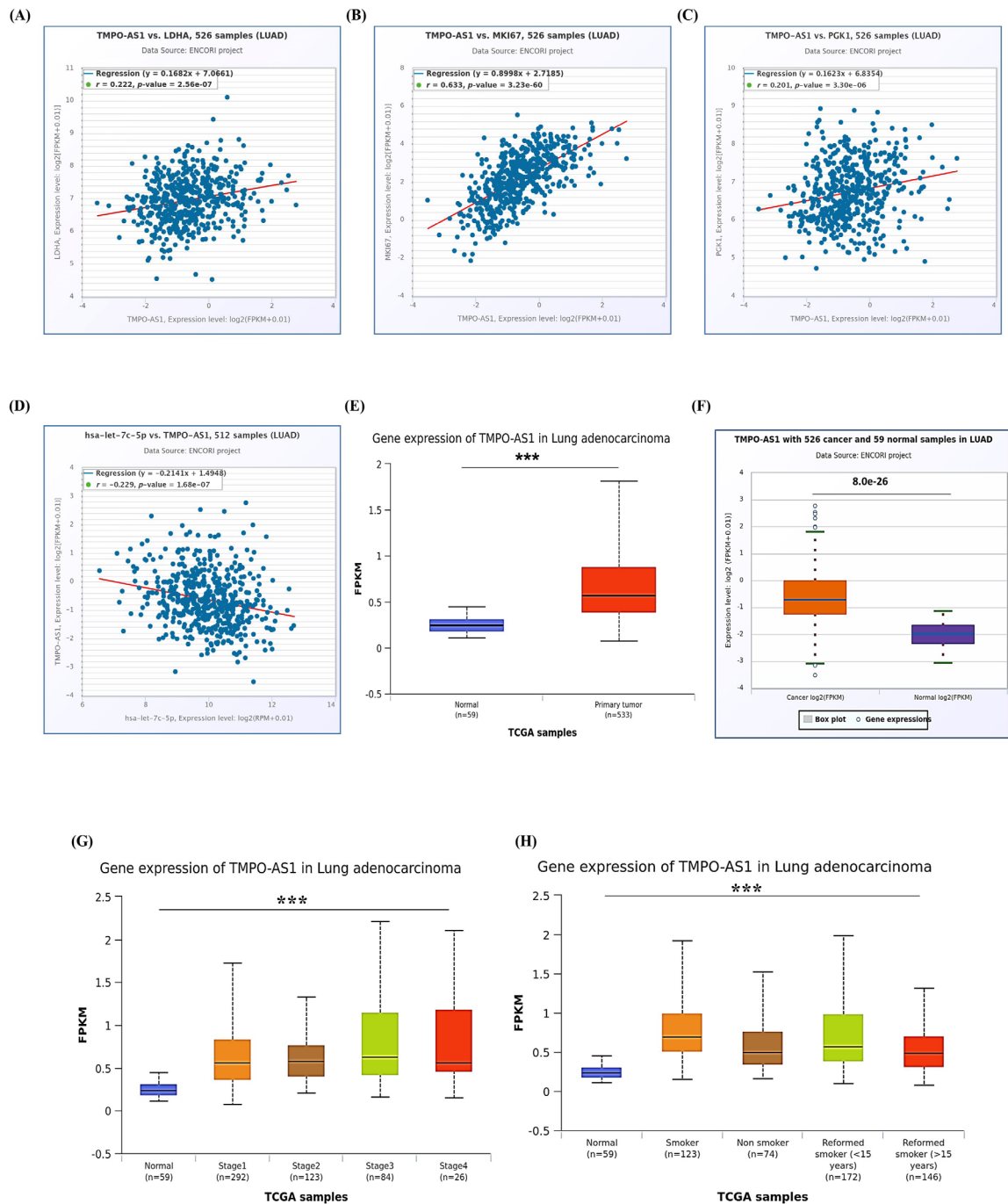


Figure 7. (A-D) Correlation between lncRNA *TMPO-AS1* expression with genes and miRNA in lung adenocarcinoma using ENCORI. (A) positive correlation between *TMPO-AS1* and *LDHA* (n=526), (B) positive correlation between *TMPO-AS1* and *MKI67* (n=526), (C) positive correlation between *TMPO-AS1* and *PGK1* (n=526), (D) negative correlation between *hsa-let-7c* and *TMPO-AS1*. Boxplot of individual gene expression of *TMPO-AS1* in lung adenocarcinoma using (E) UALCAN, (F) ENCORI. Using UALCAN to determine gene expression of *TMPO-AS1* in LUAD based on (G) individual stages and (H) smoking status.

let-7c-5p in LUAD patients, as confirmed by multiple databases, suggests its potential regulatory molecule for *LDHA*. The negative correlation observed between *hsa-let-7c-5p* and *LDHA* expression, as well as other related genes, highlights the possibility of *hsa-let-7c-5p* playing a crucial role in the regulation of *LDHA* and its associated pathways. Further investigation into the functional mechanisms of *hsa-let-7c-5p* could provide valuable insights into the development and progression of LUAD. Indeed, prediction by miRTarbase demonstrate potential

binding sites for *hsa-let-7c-5p* in *LDHA* gene.

Feedback loop between lncRNA-*TMPO-AS1* and *hsa-let-7c-5p*

Then, we examined the interactions between *hsa-let-7c-5p* miRNA and lncRNAs to construct a competing endogenous RNA (ceRNA) network. We found the LncTarD 2.0 database identified several lncRNAs significantly associated with lung cancer patients, including *SPRY4-IT1*, *HOTAIR*, *MALAT1*, *DSCAM*-

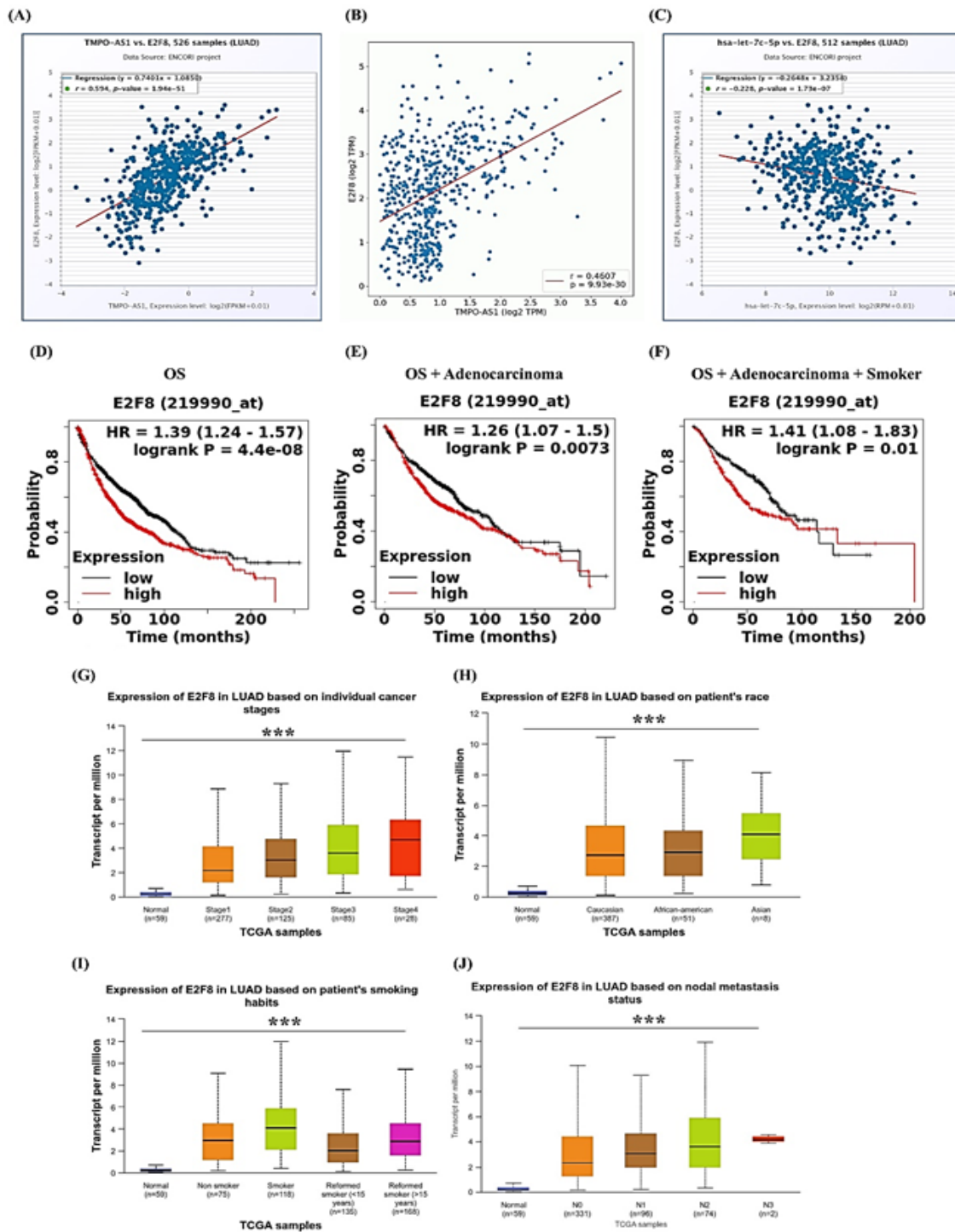


Figure 8. Transcriptional Regulation Analysis of E2F8 and Its Positive Correlation with (A-B) TMPO-AS1 Using (A) ENCORI ($r = 0.594$), (B) OncoDB ($r = 0.4607$), but negative correlation with hsa-let-7c-5p ($r = -0.228$) using ENCORI. Survival analysis of *E2F8* using KM Plotter by analyzing (D) OS in NSCLC patients (E) OS in LUAD patients, and (F) OS in smoker LUAD patients. (G-J) Expression of E2F8 in LUAD based on (G) individual cancer stages, (H) patient's race, (I) smoking history, and (J) nodal metastasis status.

AS1, BCAR4, HCP5, DANCR, LINC00922, ST8SIA6-AS1, ROR, LINC00460, NEAT 1, Linc8087, TINCR, LINP1, TMPO-AS1, CYTOR, HULC, EPIC1, NNT-AS1, EZR, PVT1, ATB, NEAT1, AC078883.3, MEG3, XIST, FENDRR, and LINC-PINT. However, the ENCORI database revealed that *LDHA* correlated positively with TMPO-AS1 ($r = 0.222$ and $p = 2.56e-07$), *MKI67* correlated positively with TMPO-AS1 ($r = 0.633$ and $p =$

$3.23e-60$), and *PGK1* correlated positively with TMPO-AS1. Importantly, as shown in Figure 7A-D, TMPO-AS1 negatively correlated with let-7c-5p ($r = -0.229$ and $p = 1.68e-07$). This suggests that TMPO-AS1 can interact with let-7c-5p, reducing their regulatory effect on mRNA gene expression. The UALCAN and ENCORI databases found a strong link between TMPO-AS1 and people with lung cancer. Figure 7E-H shows that overexpression of TMPO-

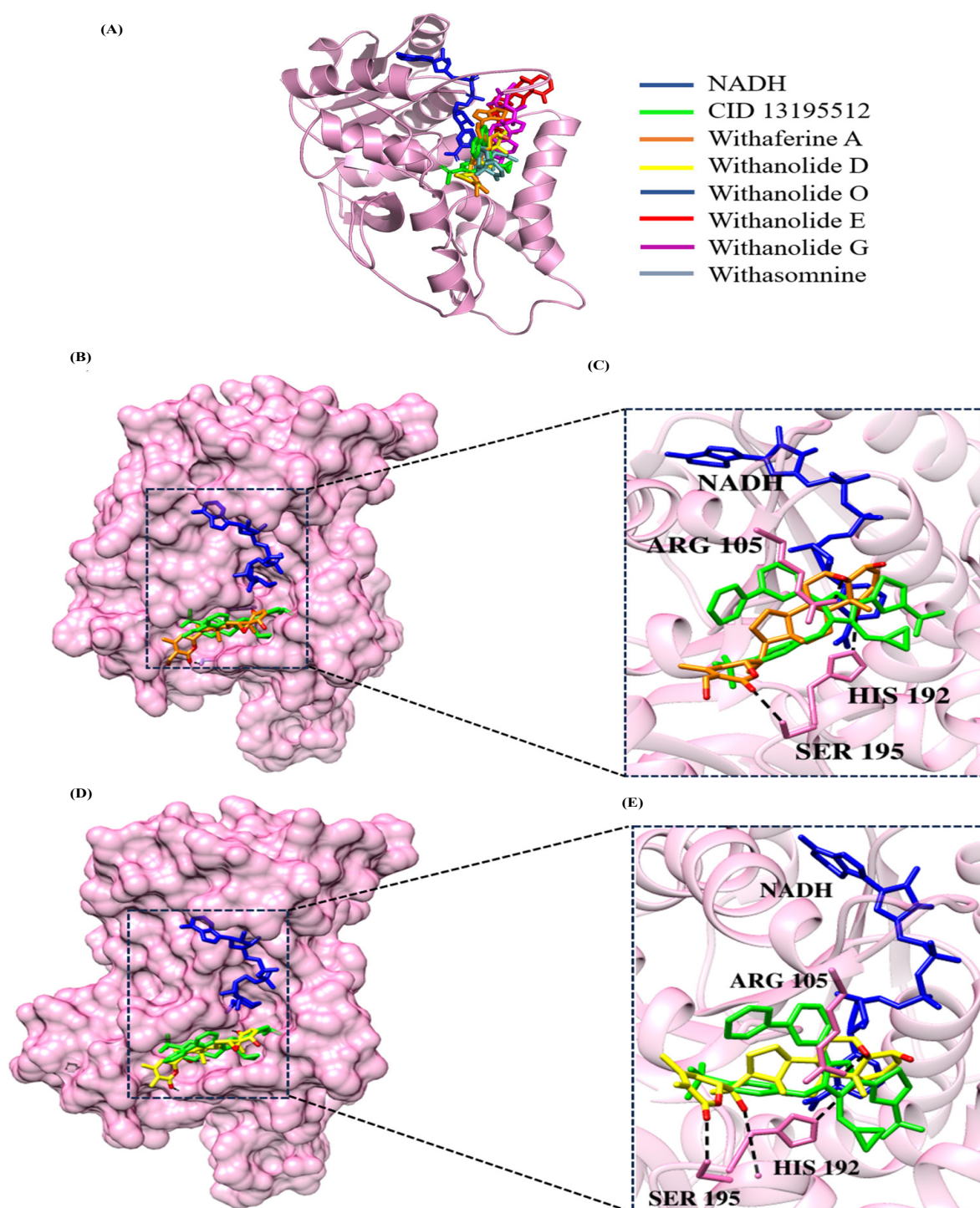


Figure 9. Human *LDHA* in complex with cofactor NADH (blue), reference inhibitor (Pubchem CID 131955127, green) and withanolides in the binding pocket. (B-E) *LDHA* interaction with Withaferin A (orange) and withanolide D (yellow) within the pocket. Zoom out views display the interactions (dashed lines) of withaferin A and withanolide D with active site residues Arg105, His192 and Ser 195.

Table 6. Binding Affinities between *LDHA* and Ligands

Inhibitors	Binding Energy (Kcal/mol)
Withanolide D +NADH	-10
Withaferine A + NADH	-9.3
Withanolide O + NADH	-9.1
Withanolide E + NADH	-8.9
Withanolide G +NADH	-8.9
Withasomnine +NADH	-6.3

AS1 was seen in smokers and people with different stages of LUAD. According to the available data, it is believed that the TMPO-AS1/hsa-let-7c-5p/*LDHA*/*MKI67*/*PGK1* feedback loop plays a role in lung cancer progression.

The transcriptional regulation of the LDHA gene

E2F transcription factors are vital to regulating cell activity and tumor growth. A study on lung cancer patients found increased expression of E2Fs such as 1, 2, 4, 5, 6, 7, and 8 in LUAD tissues. According to Table 5, only the

E2F8 transcription factor is strongly associated with the *LDHA* gene in LUAD patients. Figure 8A-C shows a strong positive association between E2F8 and the *TMPO-AS1* genes but a negative association with the *hsa-let-7c-5p* miRNA. Overexpression of E2F8 is associated with poor OS in lung cancer patients, particularly in LUAD and smokers (Figure 8 D-F). We also validated our results using the UALCAN database and saw that E2F8 is significantly overexpressed in smoker LUAD patients, including those with node metastasis, Asian (race), and adenocarcinoma stages (Figure 8G-J). E2F8, along with *LDHA/TMPO-AS1* and *hsa-let-7c-5p*, may be a potential ceRNA network that can regulate the progression of tumors and serve as prognostic predictors in LUAD patients. The fact that E2F8 and the *hsa-let-7c-5p* gene are negatively linked suggests that E2F8 expression may attenuate the expression of *hsa-let-7c-5p*.

Analysis of protein-ligand interaction between LDHA inhibitors and Withanolide

In silico docking and interactions of Withania somnifera bioactive molecules were studied to identify potential competitive inhibitors of *LDHA*. Six molecules were docking in the presence and absence of cofactor NADH. All the binding energies are mentioned in Table 6. It is observed that binding affinities and interactions were improved in the presence of NADH. We also used a potent pyrazole based reported *LDHA* inhibitor Pubchem CID 131955127 (Pubmed HYPERLINK "https://www.rcsb.org/search?q=rcsb_pubmed_container_identifiers.pubmed_id:29120638" 29120638) as a reference to compare the binding of withanolides. Best energies were observed in the case of withaferine A (-9.3 Kcal/mol) and withanolide D (-10 Kcal/mol). Binding interactions and poses of these two molecules were analyzed further to understand their interactions within the binding cavity. Withaferine A is engaged in hydrogen binding interactions with active site residues Arg105, Ser195, and His192 and hydrophobic contacts with Pro138, Ile141, Tyr238, Ile241, and Ile325. Withanolide D forms a strong interaction with *LDHA*. It forms four hydrogen bonds within the binding cavity which includes two hydrogen bonds with Arg105 and Ser195 and two hydrogen bonds with His192. The binding modes show ligands interacting within the substrate binding cavity, which is also the same for the reference inhibitor (PubChem CID 131955127). Docking and interactions of complexes are shown in Figure 9 (A-E).

Discussion

Lactate dehydrogenase (LDH) is a crucial enzyme in tumor cells that is involved in the production of lactic acid. Overexpression of *LDHA* in tumors leads to lactic acid accumulation, releasing lactate in the TME, which is associated with tumor proliferation and growth [14]. High *LDHA* expression in lung cancer patients suggests a potential role for *LDHA* in tumorigenesis and progression. This suggests that further research into the mechanisms underlying *LDHA* overexpression and its impact on cancer metabolism could lead to targeted therapies and improved

treatment strategies. High *LDHA* expression promotes aerobic glycolysis and inhibits oxidative phosphorylation, providing cancer cells with energy for rapid proliferation but also contributing to tumor progression, invasion, and resistance to therapy. Understanding these mechanisms could help identify novel therapeutic targets and improve treatment outcomes for lung cancer patients. However, owing to their high dosage and low potency, most glycolytic inhibitors available in the market could potentially lead to system toxicity [10, 14, 37]. Thus, it is vital to identify specific glycolytic inhibitors with increased potencies and low toxicity [38]. It has been observed that only intense anaerobic exercise can result in myoglobinuria due to hereditary *LDHA* deficiency, indicating that small molecules that inhibit *LDHA* enzymatic activity could be a safe chemotherapeutic agent [39]. Depending on their different growth conditions and cell types, cancer cells exhibit varying degrees of enhanced glycolysis. While normal cells generate most of their ATP through mitochondrial oxidative phosphorylation under aerobic conditions, some tumor cells tend to produce 60% of their ATP through glycolysis [40]. This increased dependence on the glycolytic pathway may serve as a basis for developing therapeutic strategies to kill cancer cells [38]. The study aimed to analyze the effects of *LDHA* overexpression in lung cancer using TIMER and the UALCAN database. Results showed that overexpression of *LDHA* in LUAD correlates with higher metastatic potential. Patients with LUSC and LUAD showed higher levels of *LDHA* gene expression, with about a 9-fold increase in expression pattern between normal and cancerous tissue. The patients with high *LDHA* expression had a poor prognosis, with a significant association with OS and FP but not PPS. The UALCAN database corroborated the findings, showing a positive correlation ($P < 0.05$) between nodal status, smoking habits, and *LDHA* gene expression level in LUAD along all stages. The upregulation of *LDHA* could be due to the promoter hypomethylation of *LDHA* in tumor tissues. An increased *LDHA* level in lung cancer cells aids in metastasis and the transition from epithelial-to-mesenchymal cells, making them resistant to available therapies. Two co-expressed genes of *LDHA*, *MKI67*, and *PGK1* were highly upregulated and associated with the poor survival outcome of LUAD patients.

miRNAs are essential in controlling biological processes like cell division, differentiation, angiogenesis, migration, apoptosis, and oncogenesis [41]. They are found in introns or exons of protein-coding genes and intergenic regions. miRNA-based cancer treatment strategies involve suppressing oncomiRNAs and upregulating tumor suppressor miRNAs [42]. miRNAs are readily available for study due to their high biological stability. They can be used as prognostic and predictive biomarkers, aiding in early diagnosis and discrimination between cancer patients and healthy individuals. In this study, *hsa-let-7c-5p* was found to be negatively associated with *LDHA*, even with *MKI67* and *PGK1*, in lung cancer patients. Receiver operator curve analysis for *hsa-let-7c* showed an AUC value of 0.95, suggesting that *hsa-let-7c* may be a regulatory molecule of *LDHA*. LncRNAs are

emerging crucial regulators of tumor progression and can interact with miRNAs as well as mRNA. LncRNAs can inhibit glycolysis by downregulating *LDHA* protein levels and thereby enhance radiosensitivity in cutaneous malignant melanoma cells [43]. Our study showed a positive correlation of TMPO-AS1 with *LDHA* and a negative correlation with let-7c-5p in LUAD. TMPO-AS1/hsa-let-7c-5p/*LDHA* ceRNA network is believed to play a crucial role in lung cancer progression and could serve as a prognostic indicator. A previous study has shown that TMPO-AS1 could regulate STRIP2 expression in LUAD by sponging let-7c-5p and serve as a prognostic biomarker [44] miR-16-5p has been shown to regulate aerobic glycolysis by targeting *LDHA* [36]. Similarly, let-7b-5p inhibits breast cancer growth and aerobic glycolysis by targeting hexokinase 2 [45]. On the other hand, TMPO-AS1 has been shown to promote esophageal cancer by regulating TMPO transcription [46]. LncRNAs interact with transporters involved in glycolysis or metabolic enzymes, influencing glycolytic metabolism and cancer progression. Further research is needed to experimentally validate the direct interaction of TMPO-AS1 with let-7c-5p and *LDHA* and their role in aerobic glycolysis.

There is evidence that hsa-let-7c-5p can inhibit tumor growth. This negative link suggests that higher levels of E2F8 may promote tumor growth and metastasis by inhibiting hsa-let-7c-5p. The study found a strong association between E2F8 and the *LDHA* gene, as well as with the TMPO-AS1 genes. These findings suggest that targeting E2F8, along with *LDHA* and TMPO-AS1, could be a potential therapeutic approach for LUAD patients. E2F8, *LDHA*, and TMPO-AS1 may act together to promote tumor growth and progression in LUAD patients. By blocking the effects of hsa-let-7c-5p on tumor-suppressing properties, E2F8 may play a part in the disruption of cell activity and the loss of tumor-suppressing properties. Also, E2F8 is strongly linked to the *LDHA* gene, which means that targeting E2F8, *LDHA*, and TMPO-AS1 could possibly stop important pathways that help tumors grow and change. This makes them promising therapeutic targets for people with LUAD.

E2F family components have been linked to various types of cancer, including bladder, lung, breast, prostate, and ovarian cancer [47–49]. *LDHA*, a direct transcriptional target of E2F1, was significantly overexpressed in metastatic LUAD tissues and played a crucial role in epithelial-mesenchymal-transition, promoting cell migration and invasion. E2F transcription factors are vital for regulating cell activity and tumor growth. A study on lung cancer patients found increased expression of E2F1/2, 4, 5, 6, 7, and 8 in LUAD tissues. The E2F8 transcription factor is strongly associated with the *LDHA* gene in LUAD patients and is positively linked with the *TMPO-AS1* genes but negatively associated with the hsa-let-7c-5p gene. Overexpression of E2F8 has been associated with LUAD patients. Collectively, E2F8/*LDHA*/TMPO-AS1 and hsa-let-7c-5p may be potential therapeutic targets for LUAD patients.

Strategies to target LDH for therapeutic intervention in LUAD include developing small-molecule inhibitors, using RNA interference or gene editing techniques, and

exploring combination therapies targeting LDH along with other metabolic pathways or signaling pathways implicated in LUAD progression. Withanolides, primarily derived from *Withania* genus are based on the ergostane skeleton. Withanolides have shown anti-cancer activities in several cancer cell lines and animal models of cancers. Withanolide-*LDHA* complexes, particularly withaferine A and withanolide D, could be prominent scaffolds for developing small-molecule inhibitors to decrease LDH activity and thereby could be tested as adjuvant therapy.

In conclusion, The study reveals that *LDHA* is overexpressed in lung cancer tissues compared to normal tissues, and high expression of *LDHA* levels associate with poor OS and first progression outcomes in NSCLC. We identified 11 key genes co-expressed with *LDHA* out of them two genes *MKI67* and *PGK1* showed positive correlation with *LDHA* and associated poor survival outcomes in LUAD patients. Furthermore, we also identified hsa-let-7c-5p and TMPO-AS1 as potential regulator of *LDHA* in LUAD. It might be possible that TMPO-AS1- hsa-let-7c-5p-*LDHA* ceRNA network could serve as potential regulator of aerobic glycolysis in LUAD and can serve as prognostic biomarkers. Further, Withanolides can inhibit the activity of LDH and can be tested as adjuvant treatment.

Author Contribution Statement

Conception: RN, AK, SKS. Interpretation, or analysis of data: RN, PV, JS, SKS, AK. Preparation of the manuscript: RN, PV, JS, SKS, AK and, Supervision: RN, AK, SKS.

Acknowledgements

Funding Support

RN would like to thank the funding support from Manipal University Jaipur for the Enhanced Seed Grant under Endowment Fund (No. E3/2023-24/QE-04-05) and DST-FIST project (DST/2022/1012) from Govt. of India to Department of Biosciences, Manipal University Jaipur. AK would like to thank the funding support from the Indian Council of Medical Research (ICMR 5/13/93/2020/NCD-III).

Conflicts of interest

The authors declare that they have no competing interests.

References

- Sharma R. Mapping of global, regional and national incidence, mortality and mortality-to-incidence ratio of lung cancer in 2020 and 2050. *Int J Clin Oncol*. 2022;27:665–75. <https://doi.org/10.1007/s10147-021-02108-2>.
- Basumallik N, Agarwal M. Small cell lung cancer. In: *StatPearls* [internet]. Treasure Island (FL): StatPearls Publishing; 2024 [cited 2024 May 29]. Available from: <http://www.ncbi.nlm.nih.gov/books/NBK482458/>.
- Wang W, Liu H, Li G. What's the difference between lung adenocarcinoma and lung squamous cell carcinoma? Evidence from a retrospective analysis in a cohort of Chinese

- patients. *Front Endocrinol.* 2022;13:947443. <https://doi.org/10.3389/fendo.2022.947443>.
4. Chen J. A Comparative Analysis of Lung Cancer Incidence and Tobacco Consumption in Canada, Norway and Sweden: A Population-Based Study. *Int J Environ Res Public Health.* 2023;20:6930. <https://doi.org/10.3390/ijerph20206930>.
 5. Walser T, Cui X, Yanagawa J, Lee JM, Heinrich E, Lee G, et al. Smoking and Lung Cancer. *Proc Am Thorac Soc.* 2008;5:811–5. <https://doi.org/10.1513/pats.200809-100TH>
 6. Riudavets M, Garcia de Herreros M, Besse B, Mezquita L. Radon and Lung Cancer: Current Trends and Future Perspectives. *Cancers.* 2022;14:3142. <https://doi.org/10.3390/cancers14133142>.
 7. de Visser KE, Joyce JA. The evolving tumor microenvironment: From cancer initiation to metastatic outgrowth. *Cancer Cell.* 2023;41:374–403. <https://doi.org/10.1016/j.ccell.2023.02.016>.
 8. Neophytou CM, Panagi M, Stylianopoulos T, Papageorgis P. The Role of Tumor Microenvironment in Cancer Metastasis: Molecular Mechanisms and Therapeutic Opportunities. *Cancers.* 2021;13:2053. <https://doi.org/10.3390/cancers13092053>.
 9. Singh L, Nair L, Kumar D, Arora MK, Bajaj S, Gadewar M, et al. Hypoxia induced lactate acidosis modulates tumor microenvironment and lipid reprogramming to sustain the cancer cell survival. *Front Oncol.* 2023;13:1034205. <https://doi.org/10.3389/fonc.2023.1034205>.
 10. Daverio Z, Balcerczyk A, Rautureau GJP, Panthu B. How Warburg-Associated Lactic Acidosis Rewires Cancer Cell Energy Metabolism to Resist Glucose Deprivation. *Cancers.* 2023;15:1417. <https://doi.org/10.3390/cancers15051417>.
 11. Lampe KJ, Namba RM, Silverman TR, Bjugstad KB, Mahoney MJ. Impact of Lactic Acid on Cell Proliferation and Free Radical Induced Cell Death in Monolayer Cultures of Neural Precursor Cells. *Biotechnol Bioeng.* 2009;103:1214–23. <https://doi.org/10.1002/bit.22352>.
 12. Qin Z, Zheng X, Fang Y. Long noncoding RNA TMPO-AS1 promotes progression of non-small cell lung cancer through regulating its natural antisense transcript TMPO. *Biochem Biophys Res Commun.* 2019;516:486–93. <https://doi.org/10.1016/j.bbrc.2019.06.088>.
 13. Sui Z, Sui X. Long non-coding RNA TMPO-AS1 promotes cell proliferation, migration, invasion and epithelial-to-mesenchymal transition in gallbladder carcinoma by regulating the microRNA-1179/E2F2 axis. *Oncol Lett.* 2021;22:855. <https://doi.org/10.3892/ol.2021.13116>.
 14. Feng Y, Xiong Y, Qiao T, Li X, Jia L, Han Y. Lactate dehydrogenase A: A key player in carcinogenesis and potential target in cancer therapy. *Cancer Med.* 2018;7:6124–36. <https://doi.org/10.1002/cam4.1820>.
 15. Liao M, Yao D, Wu L, Luo C, Wang Z, Zhang J, et al. Targeting the Warburg effect: A revisited perspective from molecular mechanisms to traditional and innovative therapeutic strategies in cancer. *Acta Pharm Sin B.* 2024;14:953–1008. <https://doi.org/10.1016/j.apsb.2023.12.003>.
 16. Choudhary MI, Yousuf S, Rahman AU. Withanolides: Chemistry and antitumor activity. *Natural Products.* Ramawat KG, Merillon JM ed. (Berlin, Heidelberg: Springer-Verlag). 2013:3465-95.
 17. Chandrashekar DS, Basha B, Balasubramanya SAH, Creighton CJ, Ponce-Rodriguez I, Chakravarthi BVSK, et al. UALCAN: A Portal for Facilitating Tumor Subgroup Gene Expression and Survival Analyses. *Neoplasia.* 2017;19:649–58. <https://doi.org/10.1016/j.neo.2017.05.002>.
 18. Li T, Fu J, Zeng Z, Cohen D, Li J, Chen Q, et al. TIMER2.0 for analysis of tumor-infiltrating immune cells. *Nucleic Acids Res.* 2020;48:W509–14. <https://doi.org/10.1093/nar/gkaa407>.
 19. Li JH, Liu S, Zhou H, Qu LH, Yang JH. starBase v2.0: decoding miRNA-ceRNA, miRNA-ncRNA and protein–RNA interaction networks from large-scale CLIP-Seq data. *Nucleic Acids Res.* 2014;42:D92–7. <https://doi.org/10.1093/nar/gkt1248>.
 20. Tang G, Cho M, Wang X. OncoDB: an interactive online database for analysis of gene expression and viral infection in cancer. *Nucleic Acids Res.* 2022;50:D1334–9. <https://doi.org/10.1093/nar/gkab970>.
 21. Tang Z, Kang B, Li C, Chen T, Zhang Z. GEPIA2: an enhanced web server for large-scale expression profiling and interactive analysis. *Nucleic Acids Res.* 2019;47:W556–60. <https://doi.org/10.1093/nar/gkz430>.
 22. Györfy B. Transcriptome-level discovery of survival-associated biomarkers and therapy targets in non-small-cell lung cancer. *Br J Pharmacol.* 2024;181:362–74. <https://doi.org/10.1111/bph.16257>.
 23. Yuan H, Yan M, Zhang G, Liu W, Deng C, Liao G, et al. CancerSEA: a cancer single-cell state atlas. *Nucleic Acids Res.* 2019;47:D900–8. <https://doi.org/10.1093/nar/gky939>
 24. Bartha Á, Györfy B. TNMplot.com: A Web Tool for the Comparison of Gene Expression in Normal, Tumor and Metastatic Tissues. *Int J Mol Sci.* 2021;22:2622. <https://doi.org/10.3390/ijms22052622>.
 25. Zhao L, Wu X, Li T, Luo J, Dong D. ctcRbase: the gene expression database of circulating tumor cells and microemboli. *Database J Biol Databases Curation.* 2020;2020:baaa020. <https://doi.org/10.1093/database/baaa020>.
 26. Uhlen M, Oksvold P, Fagerberg L, Lundberg E, Jonasson K, Forsberg M, et al. Towards a knowledge-based Human Protein Atlas. *Nat Biotechnol.* 2010;28:1248–50. <https://doi.org/10.1038/nbt1210-1248>.
 27. Kuleshov MV, Jones MR, Rouillard AD, Fernandez NF, Duan Q, Wang Z, et al. Enrichr: a comprehensive gene set enrichment analysis web server 2016 update. *Nucleic Acids Res.* 2016;44:W90–7. <https://doi.org/10.1093/nar/gkw377>.
 28. Liu CJ, Hu FF, Xie GY, Miao YR, Li XW, Zeng Y, et al. GSCA: an integrated platform for gene set cancer analysis at genomic, pharmacogenomic and immunogenomic levels. *Brief Bioinform.* 2023;24:bbac558. <https://doi.org/10.1093/bib/bbac558>.
 29. Zhao H, Yin X, Xu H, Liu K, Liu W, Wang L, et al. LncTarD 2.0: an updated comprehensive database for experimentally-supported functional lncRNA-target regulations in human diseases. *Nucleic Acids Res.* 2023;51:D199–207. <https://doi.org/10.1093/nar/gkac984>.
 30. Schrödinger L, DeLano, W. PyMOL [Internet]. 2020. Available from: <http://www.pymol.org/pymol>.
 31. Kim S, Chen J, Cheng T, Gindulyte A, He J, He S, et al. PubChem 2023 update. *Nucleic Acids Res.* 2023;51:D1373–80. <https://doi.org/10.1093/nar/gkac956>.
 32. Pettersen EF, Goddard TD, Huang CC, Couch GS, Greenblatt DM, Meng EC, et al. UCSF Chimera—A visualization system for exploratory research and analysis. *J Comput Chem.* 2004;25:1605–12. <https://doi.org/10.1002/jcc.20084>
 33. Morris GM, Huey R, Lindstrom W, Sanner MF, Belew RK, Goodsell DS, et al. AutoDock4 and AutoDockTools4: Automated docking with selective receptor flexibility. *J Comput Chem.* 2009;30:2785–91. <https://doi.org/10.1002/jcc.21256>.
 34. Morris GM, Huey R, Olson AJ. Using AutoDock for Ligand-Receptor Docking. *Curr Protoc Bioinforma.* 2008;24:8.14.1–8.14.40. <https://doi.org/10.1002/0471250953.bi0814s24>.
 35. Laskowski RA, Swindells MB. LigPlot+: Multiple Ligand–Protein Interaction Diagrams for Drug Discovery. *J Chem*

- Inf Model. 2011;51:2778–86. <https://doi.org/10.1021/ci200227u>.
36. Arora S, Singh P, Tabassum G, Dohare R, Syed MA. miR-16-5p regulates aerobic glycolysis and tumorigenesis of NSCLC cells via LDH-A/lactate/NF- κ B signaling. *Life Sci.* 2022;304:120722. <https://doi.org/10.1016/j.lfs.2022.120722>.
 37. Mishra D, Banerjee D. Lactate Dehydrogenases as Metabolic Links between Tumor and Stroma in the Tumor Microenvironment. *Cancers.* 2019;11:750. <https://doi.org/10.3390/cancers11060750>.
 38. Stine ZE, Schug ZT, Salvino JM, Dang CV. Targeting cancer metabolism in the era of precision oncology. *Nat Rev Drug Discov.* 2022;21:141–62. <https://doi.org/10.1038/s41573-021-00339-6>.
 39. Serrano-Lorenzo P, Rabasa M, Esteban J, Hidalgo Mayoral I, Domínguez-González C, Blanco-Echevarría A, et al. Clinical, Biochemical, and Molecular Characterization of Two Families with Novel Mutations in the *LDHA* Gene (GSD XI). *Genes.* 2022;13:1835. <https://doi.org/10.3390/genes13101835>.
 40. Shiratori R, Furuichi K, Yamaguchi M, Miyazaki N, Aoki H, Chibana H, et al. Glycolytic suppression dramatically changes the intracellular metabolic profile of multiple cancer cell lines in a mitochondrial metabolism-dependent manner. *Sci Rep.* 2019;9:18699. <https://doi.org/10.1038/s41598-019-55296-3>.
 41. Xiong B, Huang Q, Zheng H, Lin S, Xu J. Recent advances microRNAs and metabolic reprogramming in colorectal cancer research. *Front Oncol.* 2023;13:1165862. <https://doi.org/10.3389/fonc.2023.1165862>.
 42. Menon A, Abd-Aziz N, Khalid K, Poh CL, Naidu R. miRNA: A Promising Therapeutic Target in Cancer. *Int J Mol Sci.* 2022;23:11502. <https://doi.org/10.3390/ijms231911502>.
 43. Huang P, Zhu S, Liang X, Zhang Q, Luo X, Liu C, et al. Regulatory Mechanisms of LncRNAs in Cancer Glycolysis: Facts and Perspectives. *Cancer Manag Res.* 2021;13:5317–36. <https://doi.org/10.2147/CMAR.S314502>.
 44. Wang J, Yuan Y, Tang L, Zhai H, Zhang D, Duan L, et al. Long Non-Coding RNA-TMPO-AS1 as ceRNA Binding to let-7c-5p Upregulates STRIP2 Expression and Predicts Poor Prognosis in Lung Adenocarcinoma. *Front Oncol.* 2022;12:921200. <https://doi.org/10.3389/fonc.2022.921200>.
 45. Li L, Zhang X, Lin Y, Ren X, Xie T, Lin J, et al. Let-7b-5p inhibits breast cancer cell growth and metastasis via repression of hexokinase 2-mediated aerobic glycolysis. *Cell Death Discov.* 2023;9:114. <https://doi.org/10.1038/s41420-023-01412-2>.
 46. Luo XJ, He MM, Liu J, Zheng JB, Wu QN, Chen YX, et al. LncRNA TMPO-AS1 promotes esophageal squamous cell carcinoma progression by forming biomolecular condensates with FUS and p300 to regulate TMPO transcription. *Exp Mol Med.* 2022;54:834–47. <https://doi.org/10.1038/s12276-022-00791-3>.
 47. Gan Z, Abudurexiti A, Hu X, Chen W, Zhang N, Sang W. E2F3/5/8 serve as potential prognostic biomarkers and new therapeutic direction for human bladder cancer. *Medicine (Baltimore).* 2024;103:e35722. <https://doi.org/10.1097/MD.00000000000035722>.
 48. Liu X, Hu C. Novel Potential Therapeutic Target for E2F1 and Prognostic Factors of E2F1/2/3/5/7/8 in Human Gastric Cancer. *Mol Ther Methods Clin Dev.* 2020;18:824–38. <https://doi.org/10.1016/j.omtm.2020.07.017>.
 49. Xie D, Pei Q, Li J, Wan X, Ye T. Emerging Role of E2F Family in Cancer Stem Cells. *Front Oncol.* 2021;11:723137. <https://doi.org/10.3389/fonc.2021.723137>.



This work is licensed under a Creative Commons Attribution-Non Commercial 4.0 International License.